

## OPEN

# Robotic-Assisted Navigation for Stereotactic Neurosurgery: A Cadaveric Investigation of Accuracy, Time, and Radiation

William Anderson, MA, MD, PhD\*, Francisco A. Ponce, MD<sup>‡</sup>, Michael J. Kinsman, MD<sup>§</sup>, Sepehr Sani, MD<sup>||</sup>, Brian Hwang, MD<sup>\*\*</sup>, Diana Ghinda, MD, PhD\*, Michael Kogan, MD, PhD<sup>¶</sup>, Jonathan M. Mahoney, BS<sup>‡</sup>, Dhara B. Amin, PhD<sup>#</sup>, Margaret Van Horn, PhD<sup>#</sup>, Joshua P. McGuckin, MS<sup>Ⓜ</sup><sup>#</sup>, Dominic Razo-Castaneda, BS<sup>\*\*</sup>, Brandon S. Bucklen, PhD<sup>#</sup>

\*Department of Neurosurgery, The Johns Hopkins Hospital, Baltimore, Maryland, USA; <sup>‡</sup>Department of Neurosurgery, Barrow Neurological Institute, St. Joseph's Hospital and Medical Center, Phoenix, Arizona, USA; <sup>§</sup>Neurology, University of Kansas Medical Center, Kansas City, Kansas, USA; <sup>||</sup>Department of Neurosurgery, Rush University Medical Center, Chicago, Illinois, USA; <sup>¶</sup>Department of Neurological Surgery, Thomas Jefferson University Hospitals, Philadelphia, Pennsylvania, USA; <sup>#</sup>Musculoskeletal Education and Research Center, A Division of Globus Medical, Inc., Audubon, Pennsylvania, USA; <sup>\*\*</sup>School of Biomedical Engineering, Science and Health Systems, Drexel University, Philadelphia, Pennsylvania, USA; <sup>Ⓜ</sup>Current Affiliation: Orange County Neurosurgical Associates, Laguna Hills, California, USA

**Correspondence:** Joshua McGuckin, MS, Musculoskeletal Education and Research Center (MERC), A Division of Globus Medical, Inc., 2560 General Armistead Ave., Audubon, PA 19403, USA. Email: jmcguckin@globusmedical.com

**Received,** August 14, 2023; **Accepted,** October 18, 2023; **Published Online,** December 6, 2023.

Copyright © 2023 The Author(s). Published by Wolters Kluwer Health, Inc on behalf of Congress of Neurological Surgeons. This is an open access article distributed under the terms of the Creative Commons Attribution-Non Commercial-No Derivatives License 4.0 (CCBY-NC-ND), where it is permissible to download and share the work provided it is properly cited. The work cannot be changed in any way or used commercially without permission from the journal.

**BACKGROUND AND OBJECTIVES:** Despite frequent use, stereotactic head frames require manual coordinate calculations and manual frame settings that are associated with human error. This study examines freestanding robot-assisted navigation (RAN) as a means to reduce the drawbacks of traditional cranial stereotaxy and improve targeting accuracy.

**METHODS:** Seven cadaveric human torsos with heads were tested with 8 anatomic coordinates selected for lead placement mirrored in each hemisphere. Right and left hemispheres of the brain were randomly assigned to either the traditional stereotactic arc-based (ARC) group or the RAN group. Both target accuracy and trajectory accuracy were measured. Procedural time and the radiation required for registration were also measured.

**RESULTS:** The accuracy of the RAN group was significantly greater than that of the ARC group in both target ( $1.2 \pm 0.5$  mm vs  $1.7 \pm 1.2$  mm,  $P = .005$ ) and trajectory ( $0.9 \pm 0.6$  mm vs  $1.3 \pm 0.9$  mm,  $P = .004$ ) measurements. Total procedural time was also significantly faster for the RAN group than for the ARC group ( $44.6 \pm 7.7$  minutes vs  $86.0 \pm 12.5$  minutes,  $P < .001$ ). The RAN group had significantly reduced time per electrode placement ( $2.9 \pm 0.9$  minutes vs  $5.8 \pm 2.0$  minutes,  $P < .001$ ) and significantly reduced radiation during registration ( $1.9 \pm 1.1$  mGy vs  $76.2 \pm 5.0$  mGy,  $P < .001$ ) compared with the ARC group.

**CONCLUSION:** In this cadaveric study, cranial leads were placed faster and with greater accuracy using RAN than those placed with conventional stereotactic arc-based technique. RAN also required significantly less radiation to register the specimen's coordinate system to the planned trajectories. Clinical testing should be performed to further investigate RAN for stereotactic cranial surgery.

**KEY WORDS:** Cranial, DBS, Navigation, Radiation, Robot, SEEG, Stereotactic

*Operative Neurosurgery* 00:1–8, 2023

<https://doi.org/10.1227/ons.0000000000001024>

Cranial stereotaxy is a branch of diagnostic and therapeutic neurosurgical procedures that include the insertion/implantation of deep brain stimulation (DBS) electrodes

for movement or psychiatric disorders, stereoelectroencephalographic (SEEG) electrodes for addressing epileptic disorders, biopsy needles for diagnosis of brain lesions, catheters for laser interstitial thermal therapy, or ventricular shunts to reduce intracranial pressure.<sup>1,2</sup> Regardless of procedure or implant type, reliable and accurate targeting of intracranial targets is a defining requirement for stereotaxy.<sup>3–5</sup>

Skull-fixed stereotactic head frames are used ubiquitously for immobilization of the head and precise localization of the intracranial targets (Figure 1A).<sup>6</sup> Despite their frequent use, stereotactic

**ABBREVIATIONS:** ALIC, anterior limb of the internal capsule; A-P, anterior-posterior; ARC, arc-based; DRB, dynamic reference base; F, fornix; GPI, globus pallidus internus; NAc, nucleus accumbens; RAN, robot-assisted navigation; SEEG, stereoelectroencephalographic; SC, subcallosal cingulate; STN, subthalamic nucleus; Th, thalamus; Vim, ventral intermediate nucleus of the thalamus.

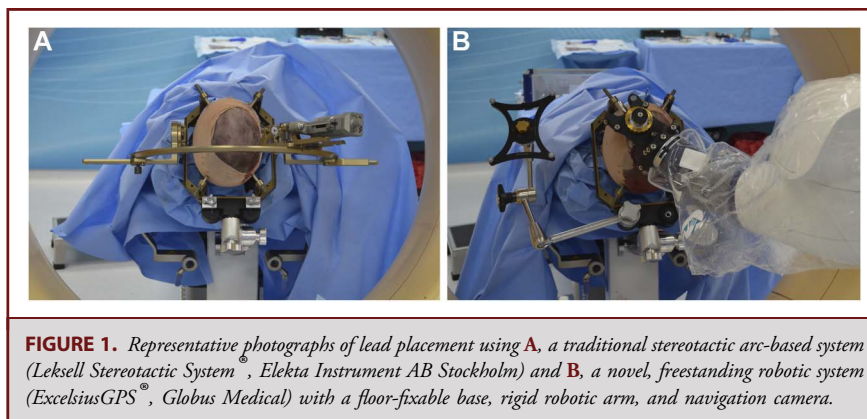


**FIGURE 1.** Representative photographs of lead placement using **A**, a traditional stereotactic arc-based system (Leksell Stereotactic System<sup>®</sup>, Elekta Instrument AB Stockholm) and **B**, a novel, freestanding robotic system (ExcelsiusGPS<sup>®</sup>, Globus Medical) with a floor-fixable base, rigid robotic arm, and navigation camera.

head frame and arc systems are considered a “tedious process”<sup>2</sup> because of coordinate calculations, manually setting the frame, and the potential for human error associated with both sequences.<sup>7,8</sup> Targeting errors have been reported in clinical studies, ranging between 1.0–3.5 mm.<sup>9–12</sup> In addition, stereotactic head frames are associated with preoperative anxiety in patients,<sup>13</sup> while clinician concerns of frame bending on targeting accuracy<sup>14</sup> may result in overtightening of the frame, increased risk of pain,<sup>15</sup> and bleeding and infection at the site of placement.<sup>16</sup> Ergonomic factors such as static postural fatigue of the clinician have also been shown to adversely affect performance in lengthy procedures.<sup>17</sup>

Alternatively, this study examines freestanding robot-assisted navigation (RAN) as a means to reduce the “tedious process”<sup>2</sup> of cranial stereotaxy and improve targeting accuracy. Robotic stereotaxy aims to automate and refine the field of functional neurosurgery. This study investigates target accuracy, operative times, and radiation exposure of a conventional stereotactic arc-based technique (Figure 1A) and a novel, freestanding robotic system (Figure 1B). The authors hypothesize that the use of RAN significantly reduces surgical time and required radiation while improving accuracy compared with arc-based systems.

## METHODS

### Specimen Preparation

Seven human torsos with heads were used in this investigation (age  $64.4 \pm 10.2$  years). Specimens were selected based on radiography to exclude specimens with trauma, deformities, or prior cranial procedures that would otherwise affect the outcomes of the study. Magnetic resonance (MR) and computed tomography (CT) scans, representing diagnostic scans that would be performed clinically, were performed on the head of each specimen before testing. All specimens were stored at  $-20^{\circ}\text{C}$  until testing.

### Surgical Procedure

Seven fellowship-trained neurosurgeons participated in this study. All surgeons performed each of the 2 experimental techniques on a single

specimen (1 procedure per hemisphere of skull) that required the insertion of 16 total leads ( $n = 8$  per technique). Rigid rods (1.8-mm diameter) were used to simulate leads. These leads broadly represent the myriad of guided depth electrodes, biopsy needles, shunts, or catheter implants used across various cranial stereotactic procedures. Surgeons placed leads using the conventional stereotactic arc-based technique (ARC) in 1 hemisphere and a robotic-assisted navigation (RAN) system (ExcelsiusGPS<sup>®</sup> Cranial Module, Globus Medical) in the contralateral hemisphere.

For each specimen, experimental techniques were randomly assigned to the left and right hemispheres. Furthermore, the order in which each surgeon performed the experimental techniques was randomly assigned, with surgeons placing all 8 leads for the first technique before moving on to the second technique. Anatomic targets were consistent across experimental techniques. Leads were placed in the subthalamic nucleus,<sup>18</sup> globus pallidus internus,<sup>18</sup> ventral intermediate nucleus of the thalamus,<sup>18</sup> anterior limb of the internal capsule,<sup>19</sup> nucleus accumbens,<sup>20</sup> thalamus,<sup>21</sup> fornix,<sup>22</sup> and the subcallosal cingulate.<sup>23</sup> These anatomic landmarks were selected to represent a broad spectrum of common DBS and SEEG targets. For both techniques, planning of these targets was completed based on offsets from the anterior commissure to posterior commissure line, as summarized in Table 1.

On the day of the study, surgeons were given approximately 30 minutes to familiarize themselves with the workflow and equipment for each technique before starting lead placement. For both techniques, the planning stage involved planning lead targets and entry points using the diagnostic CT and MR scans. Registration began with securing the stereotactic head frame (Leksell Stereotactic System<sup>®</sup>, Elekta Instrument AB Stockholm) to the specimen’s skull. All registrations were merged with the preoperative MR and CT images, with the previously planned trajectories. Then, for each trajectory, an incision was made at the entry point, and the skull was drilled with a 2.4-mm pilot hole followed by a 6.0-mm diameter entry hole to reduce the effect of trajectory skiving, which may confound accuracy measurements. Leads were then inserted through an appropriately sized guide tube, and this process was repeated for all 8 leads for each technique. Institutional review board/ethics committee approval was not required for this study because no living human subjects were involved. All cadaveric specimens were deidentified and purchased from licensed tissue vendors.

### Conventional Stereotactic Arc Workflow

An outline of the procedural steps for planning, registration, and lead placement with a conventional stereotactic head frame is presented in

**TABLE 1. Summary of AC-PC Offsets**

Anatomic location	Acronym	Coordinate/offset from AC-PC			Disease	References
		Lateral	A-P	Vertical		
Subthalamic nucleus	STN	±12.00	−4	−4	Parkinson disease	StealthStation™ 2012 <sup>18</sup>
Globus pallidus internus	GPI	±21.00	2	−4	Dystonia	StealthStation™ 2012 <sup>18</sup>
Ventral intermediate nucleus of thalamus	Vim	±13.83	−6.29	0	Essential tremor	StealthStation™ 2012 <sup>18</sup>
Anterior limb of the internal capsule	ALIC	±14.00	6 + (1/2 * [AC-PC length])	−6	Obsessive-compulsive disorder	Nuttin 2003 <sup>19</sup>
Nucleus accumbens	NAc	±3	16	2	Obsessive-compulsive disorder	Franzini 2010 <sup>20</sup>
Thalamus	Th	±5.0	4	0	Tourette syndrome	Ackermans 2011 <sup>21</sup>
Fornix	F	±4.4	9.8	7.2	Alzheimer disease	Ponce 2016 <sup>22</sup>
Subcallosal cingulate	SC	±5.6	34.2	3	Treatment resistant depression	Hamani 2009 <sup>23</sup>

AC, anterior commissure; ALIC, anterior limb of the internal capsule; A-P, anterior-posterior; F, fornix; GPI, globus pallidus internus; NAc, nucleus accumbens; PC, posterior commissure; SC, subcallosal cingulate; STN, subthalamic nucleus; Th, thalamus; Vim, ventral intermediate nucleus of the thalamus.

Table 2. For registration, a CT localizer was attached to the stereotactic head frame and a CT scan was acquired (GE VCT 64™, General Electric). A navigation system (Stealth S7® Framelink Software, Medtronic) was then used to export frame-arc coordinates. The registration stage was completed once coordinates were exported for all 8 leads.

Lead placement began with securing the arc to the frame. After attachment, the stereotactic frame was manually positioned to each of the 5 exported coordinates for each trajectory (X-axis, Y-axis, Z-axis, ring, and arc). For each trajectory, the entry point was marked followed by incision, sequential drilling, and lead insertion through an appropriately sized guide tube.

### Robotic Stereotaxy Technique

The robotic system includes a floor-mounted base platform, patient stabilization stand, navigation camera system, and software for preoperative planning and intraoperative control of the workflow (Figures 2 and 3).<sup>24</sup> An outline of the procedural steps for planning, registration, and navigation for lead placement with the fluoroscopy workflow is presented in Figure 2 and Table 3.

All planning in the RAN group was done on the robotic system. During registration, the specimen's skull was secured to the stereotactic head frame which was connected to the patient stabilization stand. A dynamic reference

**TABLE 2. Procedural Steps for Conventional Arc-Based Stereotaxy**

Stages	Procedural steps
Planning	<ul style="list-style-type: none"> <li>• Preoperative MR and CT images</li> <li>• Plan implant target and entry</li> </ul>
Registration	<ul style="list-style-type: none"> <li>• Secure Leksell® head frame to skull</li> <li>• Attach CT localizer to Leksell® frame</li> <li>• Registration CT scan</li> <li>• Merge registration scan to MR and CT images with planned trajectories</li> <li>• Export stereotactic ring and arc coordinates</li> </ul>
Placement	<ul style="list-style-type: none"> <li>• Attach Leksell® system to patient stabilization stand</li> <li>• Manually position stereotactic arc to trajectory inputs (X-axis, Y-axis, Z-axis, ring angle, arc angle)</li> <li>• Mark entry point with surgical marker</li> <li>• Incise entry point</li> <li>• Sequential drilling (2.4-mm and 6.0-mm diameter drill bits)</li> <li>• Pierce dura</li> <li>• Insert lead</li> <li>• Postoperative O-Arm™ scan for accuracy measurements<sup>a</sup></li> </ul>

CT, computed tomography; MR, magnetic resonance.

<sup>a</sup>Not included in time or radiation measurements.

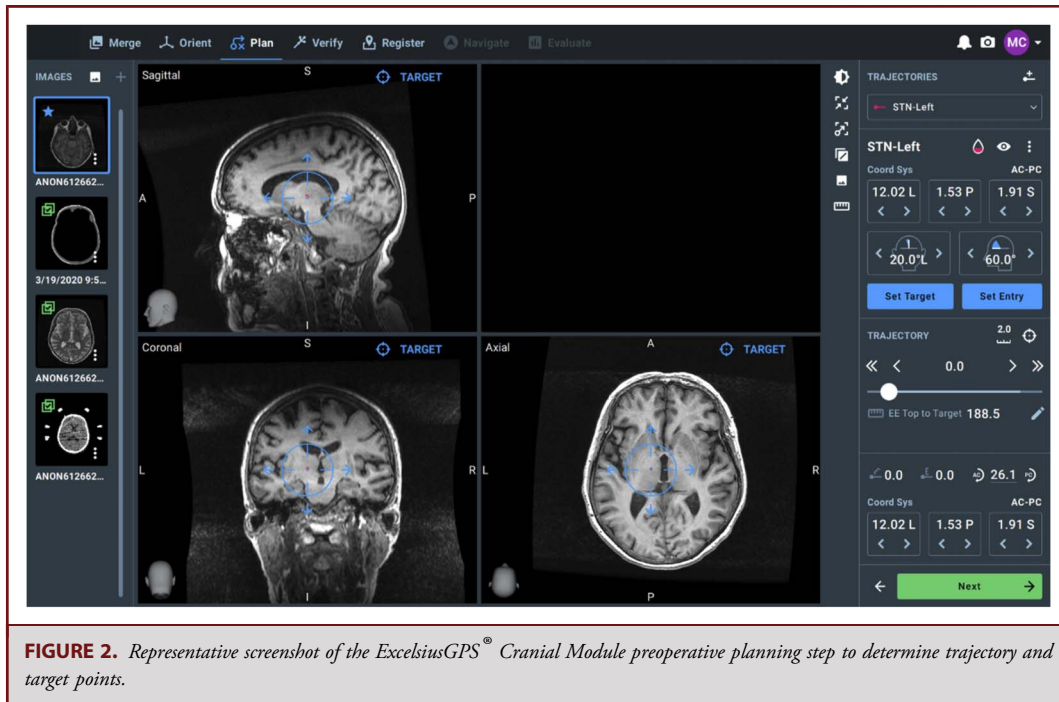


**FIGURE 2.** Representative screenshot of the ExcelsiusGPS<sup>®</sup> Cranial Module preoperative planning step to determine trajectory and target points.

base was affixed to the patient fixation and used as a reference for the robotic system. Two fluoroscopy images (coronal and sagittal), containing as much bony facial anatomy as possible and offset at least 30° from each other, were taken using a C-arm (OEC 9900 Elite, GE Healthcare) and used for registration. An anatomic landmark check with a navigated probe was used

to verify registration accuracy. Finally, the robotic base station was positioned such that all 8 planned trajectories were reachable, as determined by the navigation software. Registration was complete once reachability of all 8 planned trajectories was confirmed and the system was locked in place.

Lead placement began once the surgeon selected the first planned trajectory on the monitor. The surgeon then activated the robotic arm by stepping on a foot pedal to move the arm to the selected trajectory and down to the desired depth. The surgeon then opened passage through the end effector, locking the robotic arm in place and allowing for placement of instruments. For each trajectory, the entry point was marked followed by incision, sequential drilling, and lead insertion through an appropriately sized guide tube placed in the rigid robotic arm.

### Measurement End Points

#### Target Accuracy

After lead placement, postoperative CT scans (O-Arm<sup>™</sup>, Medtronic) were performed to assess accuracy—the distance between the planned lead and implanted lead. The postoperative CT was superimposed on the diagnostic MR and CT images used for planning. Accuracy was measured in 2 different ways to accommodate for various metrics reported in the literature: (1) the Euclidean target error and (2) the radial trajectory error (Figure 3).<sup>25</sup> Target error was defined as the distance between the planned target and the tip of the placed lead. Trajectory error was defined as the shortest distance between the planned target and the trajectory of the placed lead, perpendicular to the planned trajectory. Accuracy was reported as the mean error ± SD for each technique.

#### Operative Time

Temporal data were collected separately for registration and placement stages of each workflow. Times required to plan lead targets and trajectories were not included. The time required to complete lead placement was

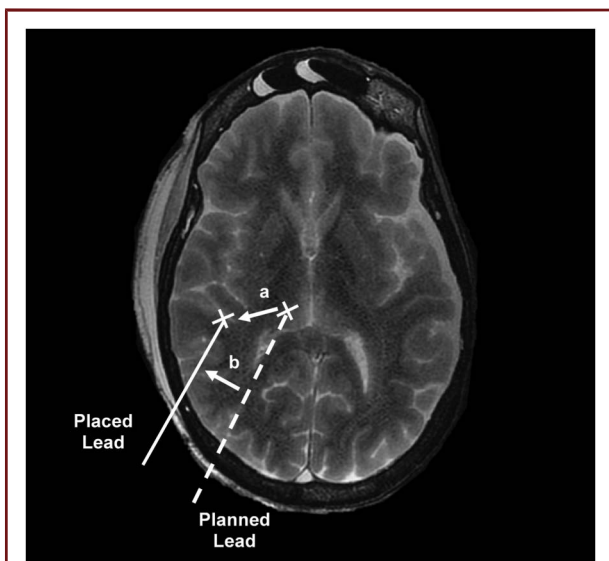


**FIGURE 3.** Representative depiction of error measurements. Target error (a) is the distance between the planned target (dashed line) and the tip of the placed lead (solid line). Trajectory error (b) is the shortest distance between the planned target and the trajectory of the placed lead perpendicular to the planned trajectory.

Downloaded from http://journals.lww.com/onsonline by BNDM5ePHkav1Eoum1tQIN4a+kLLhEZ6psHto4XIM0hCw  
CX1AWN7QpII0IH333D00dRy7T5SFACI3VVC1y0abgQZXd9Gj2mWIZLeI= on 12/06/2023

**TABLE 3. Procedural Steps for Frameless Robotic Stereotaxy With Fluoroscopy Workflow**

Stages	Procedural steps
Planning	<ul style="list-style-type: none"> <li>• Preoperative MR and CT images</li> <li>• Plan implant target and trajectory</li> </ul>
Registration	<ul style="list-style-type: none"> <li>• Secure Leksell<sup>®</sup> head frame to skull</li> <li>• Attach Leksell<sup>®</sup> head frame to patient stabilization stand</li> <li>• Position DRB next to the patient</li> <li>• Registration via coronal and sagittal fluoroscopy</li> <li>• Merge registration scans to CT image used for planning</li> <li>• Perform an anatomic landmark check to verify the merge</li> <li>• Check reachability of all planned trajectories</li> </ul>
Placement	<ul style="list-style-type: none"> <li>• Align robotic arm to planned trajectory</li> <li>• Mark entry point with surgical marker</li> <li>• Incise entry point</li> <li>• Sequential drilling (2.4-mm and 6.0-mm diameter drill bits)</li> <li>• Pierce dura</li> <li>• Insert lead</li> <li>• Postoperative O-Arm<sup>™</sup> scan for accuracy measurements<sup>a</sup></li> </ul>

CT, computed tomography; DRB, dynamic reference base; MR, magnetic resonance.  
<sup>a</sup>Not included in time or radiation measurements.

averaged by the total number of leads placed to find the average time required per lead for each technique. Time per lead, registration time, and total procedure time were compared between the 2 techniques.

### Radiation Exposure

Radiation dosages (mGy) were recorded for each technique during the registration stage. For the ARC technique, this included the registration CT scan, which was merged to the MRI used for planning to export stereotactic coordinates. For the RAN technique, this included all fluoroscopy images required to register to the preoperative CT scan. Postoperative CT scans taken for accuracy measurements were not included in the measurement of radiation exposure.

### Statistical Analysis

Statistical analysis was performed using IBM SPSS<sup>®</sup> Statistics software (SPSS<sup>®</sup> v22, IBM Corp.). A 2-tailed independent *t*-test was performed to assess differences in registration time, total procedural time, and radiation exposure between the 2 experimental techniques. An additional 2-tailed independent *t*-test was performed to assess differences in time per lead, target accuracy, and trajectory accuracy between the 2 experimental techniques. Statistical significance was defined as  $P < .05$  for all statistical comparisons.

## RESULTS

Both target error ( $P = .005$ ) and trajectory error ( $P = .004$ ) were lower for the RAN technique compared with the ARC technique

(Figure 4). The RAN group had a target error of  $1.2 \pm 0.5$  mm and trajectory error of  $0.9 \pm 0.6$  mm, while the ARC group had a target error of  $1.7 \pm 1.2$  mm and trajectory error of  $1.3 \pm 0.9$  mm.

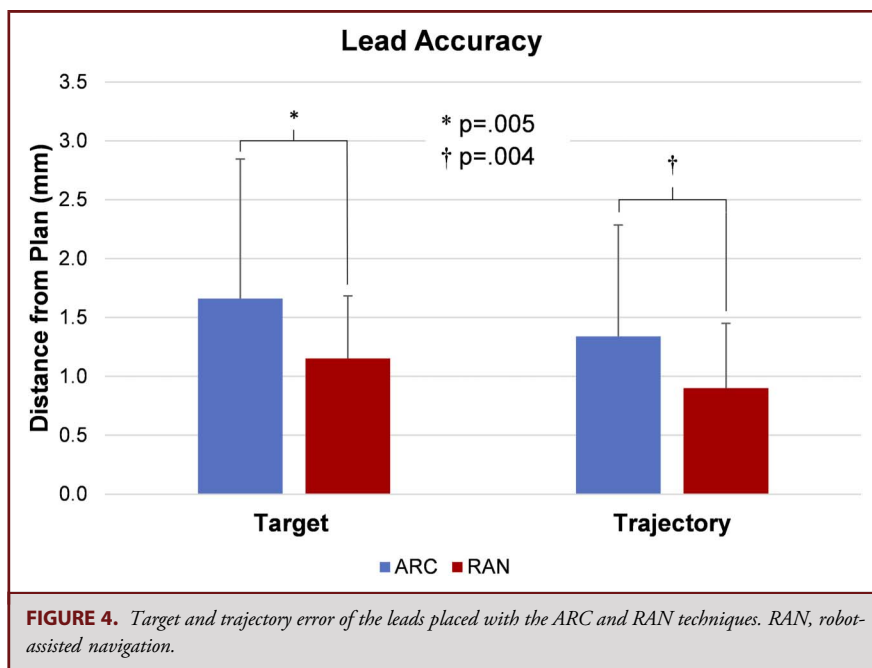
The RAN technique was also faster than the ARC technique, with significantly reduced time per lead ( $P < .001$ ), registration time ( $P < .001$ ), and total procedural time ( $P < .001$ ). Lead placement required  $2.9 \pm 0.9$  minutes per lead for the RAN group and  $5.8 \pm 2.0$  minutes per lead for the ARC group (Figure 5A). Registration time and total procedural time for the RAN group were  $21.6 \pm 5.8$  minutes and  $44.6 \pm 7.7$  minutes, respectively, and were  $37.5 \pm 3.2$  minutes and  $86.0 \pm 12.5$  minutes, respectively, for the ARC group (Figure 5B).

Finally, the radiation dose required for registration was significantly lower for the RAN technique compared with the ARC technique ( $P < .001$ ). The RAN group required  $1.9 \pm 1.1$  mGy, while the ARC group required  $76.2 \pm 5.0$  mGy.

## DISCUSSION

Traditional stereotactic head frames continue to be used widely in neurosurgical procedures, despite potential drawbacks including opportunities for human error and compromised accuracy and being time-consuming. As specialized neurosurgical procedures, including DBS and SEEG, continue to expand and advance, so too does the technology available for these procedures. RAN addresses many of the pitfalls of traditional stereotactic frames by improving targeting accuracy<sup>26</sup> and refining workflow ergonomics.<sup>17</sup> This is particularly attractive for time-consuming DBS procedures where patients are often awake.<sup>27</sup> This cadaveric study compared a RAN technique with conventional arc-based technique in target accuracy, operative times, and radiation exposure.

This study found the RAN technique to be superior to the traditional ARC technique in all 3 measured outcomes. Compared with the ARC technique, target and trajectory errors were reduced by 29% and 31%, respectively, with RAN. These results follow a similar trend to that of a recent meta-analysis that found an 11% reduction in target error using robotic assistance compared with stereotactic frames.<sup>26</sup> The authors hypothesize that improved accuracy of RAN may be due to several factors including fewer opportunities for human error in obtaining the planned trajectory and the passing of all instruments through a rigid robotic arm. However, it is important to note that while accuracy increased with RAN compared with ARC in this study, this was a difference of 0.0–1.7 mm of error depending on the surgeon. This highlights the potential accuracy of the ARC technique when used by a surgeon with sufficient experience. Therefore, the authors concluded that the accuracy benefits of RAN vs ARC are dependent on the surgeon's skill level with ARC. Although direct comparisons cannot be made to previous studies measuring DBS and SEEG electrode accuracy due to differences in methods, the error measurements in this study fall within the range of previously reported measurements.<sup>10-12,27-29</sup>

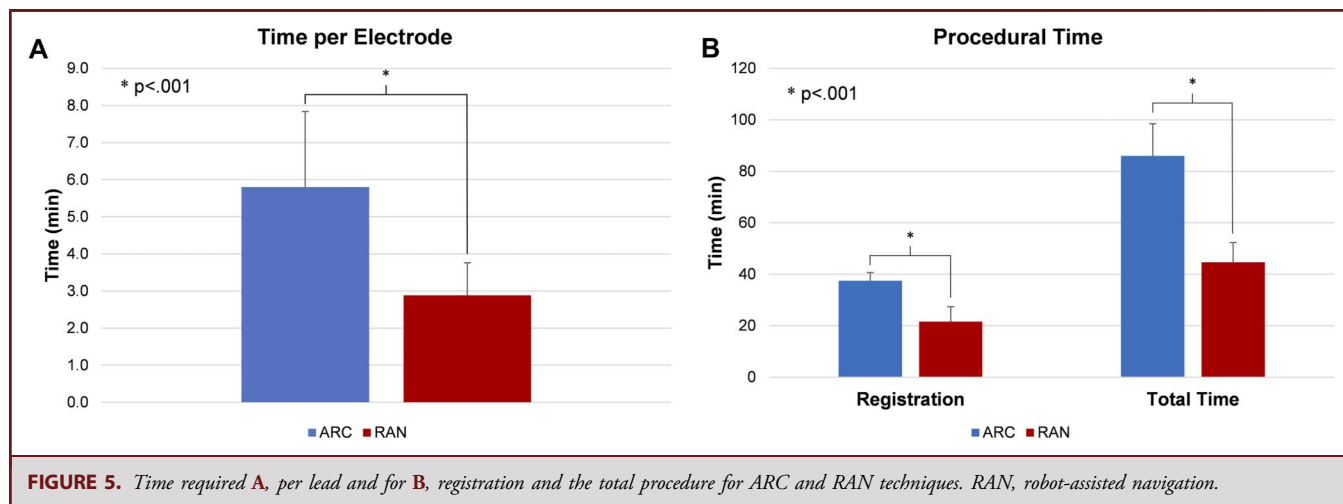


In addition, the RAN technique also required substantially less time. Total procedural time was reduced by 48% using RAN compared with the ARC technique, with a 42% shorter registration time and a 50% shorter time per lead insertion. These results are consistent with those of previous clinical studies that found faster electrode placement to be one of the greatest advantages of robot-assisted surgery.<sup>30,31</sup> In addition to requiring less time, registration for the RAN technique also required 98% less radiation than for the ARC technique.

**Limitations**

This study was limited in several ways inherent to cadaveric testing. While the targeted coordinates were chosen based on the

literature, they were not anatomically accurate because of the degradation of the cadaveric brain. For this study, accuracy measurements were made relative to the planned target and not to the actual anatomic landmark targeted. In addition, the simulated leads used in this study were rigid rods, and therefore, insertion of the leads was not perfectly representative of the true electrodes, which may be more prone to deflection in a clinical setting. Furthermore, factors including patient pain and discomfort, maintaining a sterile surgical site, use of a microelectrode recorder, and physical or cognitive tests used to determine accuracy of the electrode were not considered in this study. In addition, it is possible to use MR stereotactic coordinate determination alone without CT merging. This would reduce the amount of radiation



Downloaded from http://journals.lww.com/onsonline by BNDMfsePHKav1Zeoum1QIN4a+kLLhEZp6sIH04XIM0hCwv  
CX1AWwYQpIIQIH3D3D00dRy7TVSfACI3VC1y0abg9QZXdG9j2mWIZLeI= on 12/06/2023

used, but the effects on accuracy and efficacy compared with RAN with intraoperative CT remain speculative. In addition, the high costs required for intraoperative MRI, compatible instruments, and additional labor limit its practicality.<sup>32</sup> CT is often used as it offers the ability to merge to an MRI taken before surgery which is why it was included in this study. Finally, the controlled nature of this cadaveric study does not fully reflect of the countless variables that can potentially affect operative time in certain real-life scenarios. However, it does allow for relative comparisons between the procedural steps of RAN and ARC in a simulated surgical environment. Future cadaveric testing may compare other robotic-based or navigation-based techniques to the conventional stereotactic arc-based technique. Clinical studies are necessary to assess and compare patient outcomes.

## CONCLUSION

Stereotactic head frames and arcs remain frequently used for DBS and SEEG lead placement, despite challenges associated with human error and ergonomics. This study directly investigated time, radiation, and accuracy of lead placement in using a RAN technique compared with a conventional stereotactic arc-based technique in a cadaveric setting. The use of robotic stereotaxy resulted in greater accuracy and required less time for lead placement and less radiation than the conventional ARC technique. These trends should be studied further to investigate whether the potential advantages of RAN in stereotactic cranial surgery are observed clinically.

## Funding

This study received funding from Globus Medical, Inc. (GMI).

## Disclosures

William Anderson receives consulting fees from Globus Medical, Inc. (GMI), Iota Biosciences, and Turing Medical, royalties from GMI, and is a member of the Activity Board for Longeviti Neuro Solutions. Francisco A. Ponce receives consulting fees from GMI, Boston Scientific, and Medtronic. Sepehr Sani receives fellowship training grants from Boston Scientific, Medtronic, and Abbott, lecture and proctorship fees from Insightec, and royalties from GMI and NIH. Jonathan M. Mahoney, Dhara B. Amin, Margaret Van Horn, Joshua McGuckin, and Brandon S. Bucklen are paid employees of GMI. Jonathan M. Mahoney, Joshua McGuckin, and Brandon S. Bucklen also receive stock options from GMI. The other authors have no personal, financial, or institutional interest in any of the drugs, materials, or devices described in this article.

## REFERENCES

- Widmann G, Schullian P, Ortler M, Bale R. Frameless stereotactic targeting devices: technical features, targeting errors and clinical results. *Int J Med Robot.* 2012;8(1):1-16.
- Fomenko A, Serletis D. Robotic stereotaxy in cranial neurosurgery: a qualitative systematic review. *Neurosurgery.* 2018;83(4):642-650.
- Burchiel KJ, McCartney S, Lee A, Raslan AM. Accuracy of deep brain stimulation electrode placement using intraoperative computed tomography without micro-electrode recording. *J Neurosurg.* 2013;119(2):301-306.
- Hamid NA, Mitchell RD, Mocrift P, Westby GW, Milner J, Pall H. Targeting the subthalamic nucleus for deep brain stimulation: technical approach and fusion of pre- and postoperative MR images to define accuracy of lead placement. *J Neurol Neurosurg Psychiatry.* 2005;76(3):409-414.
- Caire F, Guehl D, Burbaud P, Benazzouz A, Cuny E. Intraoperative 3D imaging control during subthalamic deep brain stimulation procedures using O-arm<sup>®</sup> technology: experience in 15 patients. *Neurochirurgie.* 2014;60(6):276-282.
- Suh JH. Stereotactic radiosurgery for the management of brain metastases. *N Engl J Med.* 2010;362(12):1119-1127.
- Smith JA, Jivraj J, Wong R, Yang V. 30 years of neurosurgical robots: review and trends for manipulators and associated navigational systems. *Ann Biomed Eng.* 2016;44(4):836-846.
- Kwoh YS, Hou J, Jonckheere EA, Hayati S. A robot with improved absolute positioning accuracy for CT guided stereotactic brain surgery. *IEEE Trans Biomed Eng.* 1988;35(2):153-160.
- Maciunas RJ, Galloway RL, Jr., Latimer JW. The application accuracy of stereotactic frames. *Neurosurgery.* 1994;35(4):682-694; discussion 694-5.
- Dorfer C, Minchev G, Czech T, et al. A novel miniature robotic device for frameless implantation of depth electrodes in refractory epilepsy. *J Neurosurg.* 2017;126(5):1622-1628.
- González-Martínez J, Bulacio J, Thompson S, et al. Technique, results, and complications related to robot-assisted stereoelectroencephalography. *Neurosurgery.* 2016;78(2):169-180.
- Verburg N, Baayen JC, Idema S, et al. In vivo accuracy of a frameless stereotactic drilling technique for diagnostic biopsies and stereoelectroencephalography depth electrodes. *World Neurosurg.* 2016;87:392-398.
- Avbovbo UE, Appel SJ. Strategies to alleviate anxiety before the placement of a stereotactic radiosurgery frame. *J Neurosci Nurs.* 2016;48(4):224-228.
- Treuer H, Hunsche S, Hoevels M, et al. The influence of head frame distortions on stereotactic localization and targeting. *Phys Med Biol.* 2004;49(17):3877-3887.
- Wang DD, Lau D, Rolston JD, Englot DJ, Sneed PK, McDermott MW. Pain experience using conventional versus angled anterior posts during stereotactic head frame placement for radiosurgery. *J Clin Neurosci.* 2014;21(9):1538-1542.
- Ramakrishna N, Rosca F, Friesen S, Tezcanli E, Zygmanski P, Hacker F. A clinical comparison of patient setup and intra-fraction motion using frame-based radiosurgery versus a frameless image-guided radiosurgery system for intracranial lesions. *Radiother Oncol.* 2010;95(1):109-115.
- Berguer R. Surgery and ergonomics. *Arch Surg.* 1999;134(9):1011-1016.
- StealthStation<sup>TM</sup> Application. Version 2.0.1-7.* Medtronic; 2012.
- Nuttin BJ, Gabriels L, van Kuyck K, Cosyns P. Electrical stimulation of the anterior limbs of the internal capsules in patients with severe obsessive-compulsive disorder: anecdotal reports. *Neurosurg Clin N Am.* 2003;14(2):267-274.
- Franzini A, Messina G, Gambini O, et al. Deep-brain stimulation of the nucleus accumbens in obsessive compulsive disorder: clinical, surgical and electrophysiological considerations in two consecutive patients. *Neurol Sci.* 2010;31(3):353-359.
- Ackermans L, Duits A, van der Linden C, et al. Double-blind clinical trial of thalamic stimulation in patients with Tourette syndrome. *Brain.* 2011;134(Pt 3):832-844.
- Ponce FA, Asaad WF, Foote KD, et al. Bilateral deep brain stimulation of the fornix for Alzheimer's disease: surgical safety in the ADvance trial. *J Neurosurg.* 2016;125(1):75-84.
- Hamani C, Mayberg H, Snyder B, Giacobbe P, Kennedy S, Lozano AM. Deep brain stimulation of the subcallosal cingulate gyrus for depression: anatomical location of active contacts in clinical responders and a suggested guideline for targeting. *J Neurosurg.* 2009;111(6):1209-1215.
- Vaccaro AR, Harris JA, Hussain MM, et al. Assessment of surgical procedural time, pedicle screw accuracy, and clinician radiation exposure of a novel robotic navigation system compared with conventional open and percutaneous freehand techniques: a cadaveric investigation. *Global Spine J.* 2019;10(7):814-825.
- Li Z, Zhang JG, Ye Y, Li X. Review on factors affecting targeting accuracy of deep brain stimulation electrode implantation between 2001 and 2015. *Stereotact Funct Neurosurg.* 2016;94(6):351-362.
- Vakharia VN, Sparks R, O'Keeffe AG, et al. Accuracy of intracranial electrode placement for stereoelectroencephalography: a systematic review and meta-analysis. *Epilepsia.* 2017;58(6):921-932.

27. Neudorfer C, Hunsche S, Hellmich M, El Majdoub F, Maarouf M. Comparative study of robot-assisted versus conventional frame-based deep brain stimulation stereotactic neurosurgery. *Stereotact Funct Neurosurg*. 2018;96(5):327-334.
28. Brandman D, Hong M, Clarke DB. Preclinical evaluation of the stealth autoguide robotic guidance device for stereotactic cranial surgery: a human cadaveric study. *Stereotact Funct Neurosurg*. 2021;99(4):343-350.
29. Candela-Cantó S, Aparicio J, López JM, et al. Frameless robot-assisted stereoelectroencephalography for refractory epilepsy in pediatric patients: accuracy, usefulness, and technical issues. *Acta Neurochir (Wien)*. 2018;160(12):2489-2500.
30. Abel TJ, Varela Osorio R, Amorim-Leite R, et al. Frameless robot-assisted stereoelectroencephalography in children: technical aspects and comparison with Talairach frame technique. *J Neurosurg Pediatr*. 2018;22(1):37-46.
31. Miller BA, Salehi A, Limbrick DD, Jr., Smyth MD. Applications of a robotic stereotactic arm for pediatric epilepsy and neurooncology surgery. *J Neurosurg Pediatr*. 2017;20(4):364-370.
32. Guo Z, Leong MC, Su H, Kwok KW, Chan DT, Poon WS. Techniques for stereotactic neurosurgery: beyond the frame, toward the intraoperative magnetic resonance imaging-guided and robot-assisted approaches. *World Neurosurg*. 2018;116:77-87.

## COMMENTS

**B**usiness organizational experts claim 3 basic reasons to employ robots: they are better, faster, and cheaper than human labor. But are they safer? Increasingly robots are being deployed on humans by other humans—a surgeon—who acquires lonesome intraoperative experience not uncommonly through unsystematic error.

In plain words, we learn from mistakes—rarely others’—more often our own. Yet no matter how cool the tool, lean the “sigma six,” “slim the

“variance,” or wise the “advisor”—mistakes WILL accrue. Here is where the oft used metaphor of “process safety” in surgery fails. Yes of course better instruments foster faster perhaps even safer surgery, but ultimately—whatever the tool—safety solely rests in the hands of a single experienced surgeon.

This meticulous anatomic head-to-head comparison of DBS lead placement shows that robotic-assisted surgery is more accurate, faster and importantly requires less radiation exposure compared with traditional frame-based methods. Naturally, we still need postoperative clinical outcome studies in live humans to declare robotic supremacy. But do we really need a blinded neurologist to see that technology has progressed safely? Which would you choose to start your own practice? Which would Leskell have chosen?

Cooler tools may be better, faster and cheaper, but only if they are safer. Modern instruments tend to flatten learning curves and operative times but in the end they remain merely tools—subject to our judgment. Recently in this Journal another equally timely article on robotic DBS placement describes a truly excellent and safe single center experience.<sup>1a</sup> *Vita brevis* everyone... stay cool.

**Travis Tierney**  
Miami, Florida, USA

- 
- 1a. Fayed I, Smit RD, Vinjamuri S, et al. Robot-assisted minimally invasive asleep single-stage deep brain stimulation surgery: operative technique and systematic review. *Oper Neurosurg*. 2023.

PAGE INTENTIONALLY LEFT BLANK

PAGE INTENTIONALLY LEFT BLANK

PAGE INTENTIONALLY LEFT BLANK

